

# $\alpha$ 2,6-Sialic Acid on Platelet Endothelial Cell Adhesion Molecule (PECAM) Regulates Its Homophilic Interactions and Downstream Antiapoptotic Signaling<sup>\*[5]</sup>

Received for publication, October 6, 2009, and in revised form, December 24, 2009. Published, JBC Papers in Press, January 4, 2010, DOI 10.1074/jbc.M109.073106

Shinobu Kitazume<sup>‡</sup>, Rie Imamaki<sup>‡</sup>, Kazuko Ogawa<sup>‡</sup>, Yusuke Komi<sup>§</sup>, Satoshi Futakawa<sup>¶</sup>, Soichi Kojima<sup>§</sup>, Yasuhiro Hashimoto<sup>¶</sup>, Jamey D. Marth<sup>||</sup>, James C. Paulson<sup>\*\*</sup>, and Naoyuki Taniguchi<sup>‡</sup> <sup>###1</sup>

From the <sup>‡</sup>Disease Glycomics Team and <sup>§</sup>Molecular Ligand Biology Research Team, RIKEN Advanced Science Institute, 2-1 Hirosawa, Wako, Saitama 351-0198, Japan, the <sup>¶</sup>Department of Biochemistry, School of Medicine, Fukushima Medical University, 1 Hikarigaoka, Fukushima 960-1295, Japan, the <sup>||</sup>Department of Cellular and Molecular Medicine and Howard Hughes Medical Institute, University of California, San Diego, La Jolla, California 92093, the <sup>\*\*</sup>Departments of Chemical Physiology and Molecular Biology, The Scripps Research Institute, La Jolla, California 92037, and the <sup>###</sup>Department of Disease Glycomics Laboratory, Research Institute for Microbial Disease, Osaka University, Suita, Osaka 565-0871, Japan

Antiangiogenesis therapies are now part of the standard repertoire of cancer therapies, but the mechanisms for the proliferation and survival of endothelial cells are not fully understood. Although endothelial cells are covered with a glycocalyx, little is known about how endothelial glycosylation regulates endothelial functions. Here, we show that  $\alpha$ 2,6-sialic acid is necessary for the cell-surface residency of platelet endothelial cell adhesion molecule (PECAM), a member of the immunoglobulin superfamily that plays multiple roles in cell adhesion, mechanical stress sensing, antiapoptosis, and angiogenesis. As a possible underlying mechanism, we found that the homophilic interactions of PECAM in endothelial cells were dependent on  $\alpha$ 2,6-sialic acid. We also found that the absence of  $\alpha$ 2,6-sialic acid down-regulated the tyrosine phosphorylation of PECAM and recruitment of Src homology 2 domain-containing protein-tyrosine phosphatase 2 and rendered the cells more prone to mitochondrion-dependent apoptosis, as evaluated using PECAM-deficient endothelial cells. The present findings open up a new possibility that modulation of glycosylation could be one of the promising strategies for regulating angiogenesis.

Angiogenesis is a physiological process that encompasses the growth of capillary blood vessels, and the disturbance of angiogenesis contributes to the pathogenesis of numerous disorders, including cancer (1). Indeed, different types of antiangiogenic agents targeting endothelial cells have been developed as anti-cancer treatments (2). Pathological angiogenesis is predomi-

nantly driven by vascular endothelial growth factor, a proangiogenic growth factor expressed by many solid tumors (3, 4). Angiogenesis is also regulated by endothelial cell adhesion molecules, such as vascular endothelial cadherin (VE-cadherin),<sup>2</sup> integrins, and platelet endothelial cell adhesion molecule (PECAM). For integrin activation, a mechanosensory complex composed of PECAM, VE-cadherin, and vascular endothelial growth factor receptor 2 causes the initial response (5). PECAM was originally identified as a major endothelial cell adhesion molecule, but it has recently been recognized to play important roles in controlling the activation and survival of endothelial cells (6). PECAM is considered to be an inhibitory receptor, and its cytoplasmic region possesses an immunoreceptor tyrosine-based inhibitory motif that becomes tyrosine-phosphorylated and subsequently recruits and activates Src homology 2 domain-containing protein-tyrosine phosphatase 2 (SHP2) for the transduction of inhibitory signals to the cell (7). Notably, recent studies have shown that PECAM functions as an inhibitor of mitochondrion-dependent apoptosis (8–12) and regulates pathological angiogenesis (13).

Even though most endothelial cell adhesion molecules, including PECAM, are heavily glycosylated, the aspect of how endothelial glycans play roles in vascular physiology and pathology remains largely unknown. The previous observations that vascular endothelial cells express glycoproteins significantly modified with  $\alpha$ 2,6-linked sialic acid by the  $\beta$ -galactoside sialyltransferase ST6Gal I (14) and that cytokine treatments enhance ST6Gal I expression in endothelial cells (15) prompted us to study the functional roles of  $\alpha$ 2,6-linked sialic acid in normal and pathogenic angiogenesis. In this study using ST6Gal I-deficient mice, we demonstrate that in the absence of  $\alpha$ 2,6-sialic acid, PECAM was unable to remain on the cell surface and incompletely transduced inhibitory signals such as those required for its antiapoptotic role.

<sup>\*</sup> This work was supported, in whole or in part, by National Institutes of Health Grant HL57345 (to J. M.). This work was also supported by grants from the Systems Glycobiology Research Project (to N. T.), the Chemical Genomics Research Project from RIKEN (to S. Kojima), Japan Foundation for Applied Enzymology (to S. Kitazume), Yamada Science Foundation (to S. Kitazume), and Grant 18570141 from the Ministry of Education, Science, Sports and Culture of Japan (to S. Kitazume).

<sup>‡</sup> Author's Choice—Final version full access.

<sup>[5]</sup> The on-line version of this article (available at <http://www.jbc.org>) contains supplemental Figs. S1–S4.

<sup>1</sup> To whom correspondence should be addressed: Disease Glycomics Team, RIKEN Advanced Science Institute, 2-1 Hirosawa, Wako, Saitama 351-0198, Japan. Tel.: 81-48-467-9616; Fax: 81-48-467-9617; E-mail: tani@sanken.osaka-u.ac.jp.

<sup>2</sup> The abbreviations used are: VE-cadherin, vascular endothelial cadherin; Fc, hinge and constant region of IgG; GAPDH, glyceraldehyde-3-phosphate dehydrogenase; HUVEC, human umbilical vein endothelial cell; PECAM, platelet endothelial cell adhesion molecule; SHP2, Src homology 2 domain-containing protein-tyrosine phosphatase 2; SSA, *S. sieboldiana* agglutinin; ST6Gal I,  $\beta$ -galactoside  $\alpha$ 2,6-sialyltransferase; PBS, phosphate-buffered saline.

### EXPERIMENTAL PROCEDURES

**Materials**—The sources of the materials used in this study were as follows: tissue culture media and reagents, including Dulbecco's modified Eagle's medium/F-12, from Invitrogen; FuGENE 6 and recombinant *N*-glycosidase F from Roche Applied Science; protein A-Sepharose Fast Flow from GE Healthcare; protein molecular weight standards from Bio-Rad; and all other chemicals from Sigma or Wako Chemicals. Protein concentrations were determined with BCA protein assay reagents (Pierce). For detection of proteins after SDS-PAGE, 2D-Silver Stain-II (Cosmo Bio) was used. All animal experiments were performed in compliance with the Institutional Guidelines for Animal Experiments of RIKEN.

**Expression Plasmids**—Fc-tagged PECAM (Fc-PECAM) was generated by inserting mouse PECAM amino acids 1–590 into the EcoRV and SpeI sites of pEF encoding the hinge and constant region (Fc) of human IgG1 in-frame. Fc-tagged mPECAM<sub>R90A</sub> was generated using a QuikChange site-directed mutagenesis kit (Stratagene). A ViraPower adenoviral expression system (Invitrogen) was used to produce recombinant adenoviruses carrying rat ST6Gal I or control LacZ according to the manufacturer's protocol. To achieve this, a rat ST6Gal I-FLAG pcDNA was subcloned into the pENTR TOPO vector (Invitrogen). The ST6Gal I entry clone vector was used in LR clonase recombination reactions (Invitrogen) with the Gateway adenoviral backbone vector pAd/CMV/V5-DEST (Invitrogen).

**Cell Culture**—Human umbilical vein endothelial cells (HUVECs; Takara) were cultured in EBM-2 (Takara) containing 2% fetal bovine serum and EGM<sup>TM</sup>-2 SingleQuots (Takara) and used within four passages. Viral titers were determined using an Adeno-X<sup>TM</sup> rapid titer kit (Clontech). Primary liver sinusoidal endothelial cells were prepared from the livers of wild-type and ST6Gal I-deficient mice using CD146 MicroBeads (Miltenyi Biotec), according to the manufacturer's protocol, cultured in Dulbecco's modified Eagle's medium/F-12 containing 10% fetal bovine serum and 50  $\mu$ g/ml endothelial mitogen (Biomedical Technologies Inc.), and used within three passages.

**Immunofluorescence**—Mouse endothelial cells or HUVECs were grown on type I collagen-coated chamber slides (Iwaki). After fixation with 4% paraformaldehyde, treatment with 0.1% Triton X-100 for 15 min, and blocking with 5% goat serum in PBS, the cells were incubated with anti-PECAM (MEC13.3; 1:100 dilution; BD Biosciences) and anti-adaptin  $\gamma$  (1:100 dilution; BD Transduction Laboratories) or anti-EEA-1 (1:100 dilution; BD Transduction Laboratories) antibodies or an anti-lysobisphosphatidic acid antibody. The cells were then incubated with Alexa Fluor 488-conjugated anti-rat IgG (1:100 dilution; Invitrogen) and Alexa Fluor 546-conjugated anti-mouse IgG (1:100 dilution; Invitrogen), respectively. For the HUVECs, an anti-human PECAM antibody (H-300; 1:100 dilution; Santa Cruz Biotechnology) and *Sambucus sieboldiana* agglutinin (SSA)-biotin (1:100 dilution; Honen Co.) were used, followed by Alexa Fluor 546-conjugated anti-rabbit IgG (1:100 dilution; Invitrogen) and Alexa Fluor 488-conjugated streptavidin (1:100 dilution; Invitrogen). After washing with PBS, the samples were mounted in ProLong Gold antifade reagent containing 4',6-

diamidino-2-phenylindole (Invitrogen) and observed using an FV1000-D laser scanning confocal microscope (Olympus).

**Immunohistochemistry**—To prepare brain sections, mice were perfused transcardially with 0.1 M phosphate-buffered 4% paraformaldehyde, sequentially immersed in the same fixative for 16 h, phosphate-buffered 20% sucrose for 6 h, and phosphate-buffered 40% sucrose for 16 h at 4 °C, and then frozen. Sections (10- $\mu$ m thickness) were mounted on aminopropyltriethoxysilane-coated glass slides and air-dried for 15 min. For TJA-I lectin staining, we performed fluorescence-indirect tyramide signal amplification. Briefly, brain sections were incubated with 0.3% hydrogen peroxidase in methanol, treated with the blocking solutions supplied in a tyramide signal amplification kit (TSA Biotin System; PerkinElmer Life Sciences), and then incubated with anti-PECAM antibodies MEC13.3 (BD Biosciences) or M-20 (Santa Cruz Biotechnology) diluted 1:500 in TBS (0.1 M Tris-HCl, pH 7.5, 0.15 M NaCl) overnight at 4 °C. After three rinses with TNT buffer (TBS containing 0.05% Tween 20) for 5 min each, the sections were incubated with biotinylated TJA-I lectin (1:1000 dilution; Honen Co.) plus Alexa Fluor 546-conjugated goat anti-rat IgG (1:100 dilution; Molecular Probes) for 45 min. After three rinses with TNT buffer, tyramide-enhanced immunoreactivity was visualized with horseradish peroxidase-conjugated streptavidin (1:100 dilution; Invitrogen) for 45 min and Alexa Fluor 488-conjugated tyramide (1:10 dilution; Molecular Probes) for 10 min. When we performed single staining for TJA-I lectin or PECAM, each staining pattern was identical to that obtained in the double staining. To detect ST6Gal I, we performed the tyramide signal amplification method using an anti-ST6Gal I antibody (1:100 dilution; IBL-Japan Co.) and biotinylated goat anti-rabbit IgG (1:100 dilution; GE Healthcare).

**Real Time Quantitative PCR**—Total RNA was isolated from mouse lung tissues using TRIzol reagent (Invitrogen), and 5–10  $\mu$ g of the RNA was reverse-transcribed with random hexamers using a SuperScript II reverse transcription kit (Invitrogen) according to the manufacturer's protocol. Amplifications of the cDNA and the PCR conditions were described previously (16). The probes for PECAM were labeled with the fluorescent reporter dye FAM<sup>TM</sup>. The probes for glyceraldehyde-3-phosphate dehydrogenase (GAPDH) were labeled with VIC<sup>TM</sup> at their 5' ends and the quencher dye TAMRA<sup>TM</sup> at their 3' ends. The expression levels of the target gene were measured in duplicate and normalized by the corresponding GAPDH expression levels.

**Western Blotting**—Lung tissues from mice and HUVEC lysates were homogenized in T-PER Tissue Protein Extraction Reagent (Pierce) containing a protease inhibitor mixture (Roche Applied Science). The lung homogenates (10  $\mu$ g of protein), HUVEC lysates (10  $\mu$ g of protein), or immunoprecipitated samples were separated by SDS-PAGE using 4–20% gradient gels and transferred to nitrocellulose membranes. The membranes were incubated with an anti-PECAM antibody (M-20; 1:2000 dilution; Santa Cruz Biotechnology) or an anti-phosphotyrosine antibody (6E10; 1:1000 dilution; Roche Applied Science). Horseradish peroxidase-conjugated donkey anti-goat and anti-mouse IgG (1:1000 dilution; Jackson ImmunoResearch) were used as the secondary antibodies and a

SuperSignal chemiluminescent substrate (Thermo Fisher Scientific Inc.) was used for detection. As a loading control, we detected GAPDH on the same membranes using an anti-GAPDH antibody (1:1000 dilution; Chemicon) and horseradish peroxidase-conjugated goat anti-mouse IgG (1:1000 dilution; Amersham Biosciences). The detected bands for PECAM and GAPDH were quantified using a Luminoimage Analyzer LAS-1000 PLUS (Fuji Film).

**Cell-surface Biotinylation**—Liver sinusoidal endothelial cells grown on 60-mm culture plates were labeled with Sulfo-NHS-LC-Biotin (Pierce; 1 ml/ml ice-cold PBS, pH 8.0) for 30 min at 4 °C. After three washes with 0.1 M glycine in PBS, pH 8.0, and one wash with PBS, culture medium was added to the plates, and the cells were cultured for defined periods of time (0, 3, 6, 12, and 24 h).

**Flow Cytometry**—Transfection of endothelial cells was achieved by infection with adenovirus preparations for ST6Gal I or LacZ using equivalent plaque-forming units/cell. 48 h after infection, the cells were detached with 20 mM EDTA in PBS and resuspended as single cell suspensions in FACS buffer (PBS containing 1% bovine serum albumin and 0.05% sodium azide). The cells ( $5 \times 10^5$ ) were incubated with SSA-fluorescein isothiocyanate (10  $\mu$ g/ml) or an anti-PECAM-PE antibody (5  $\mu$ g/ml; Santa Cruz Biotechnology) for 30 min on ice, washed three times, and suspended in FACS buffer. Flow cytometry data were acquired using an EPICS XL cytometer (Beckman Coulter) and analyzed using the Expo32 software (Beckman Coulter).

**Immunoprecipitation and SSA Lectin Precipitation**—Lung lysates were prepared from wild-type and ST6Gal I-deficient mice. To release the PECAM complexes, the lysates were boiled in the presence of 0.5% SDS and then diluted to 0.1% SDS before immunoprecipitation. The lysates (1 mg/ml) were precleared with protein G-agarose for 30 min. After centrifugation to remove insoluble material, the supernatants (100  $\mu$ l) were incubated with 2.5  $\mu$ g of an anti-PECAM antibody (M-20) or 30  $\mu$ l of SSA-agarose (Honen Co.) for 16 h. For PECAM precipitation, 30  $\mu$ l of protein G-Sepharose was added. The precipitates were washed four times, separated by SDS-PAGE, transferred to nitrocellulose, and probed with an anti-PECAM antibody (M-20).

**In Vitro PECAM Pulldown Assay**—Fc-PECAM or Fc-PECAM<sub>R90A</sub> protein was purified from culture media obtained from COS cells transiently expressing the protein. Fc-PECAM (200 ng) absorbed onto 15  $\mu$ l of protein A-Sepharose was incubated with His-tagged PECAM (PECAM-His, 1  $\mu$ g; R&D Systems) in the presence or absence of 2 milliunits of *Vibrio cholerae* sialidase (Nacalai Tesque) in PBS for 1 h. Alternatively, Fc-PECAM that was incubated with sialidase for 1 h was washed to remove sialidase and then incubated with PECAM-His in PBS for another 1 h. The reaction mixtures were analyzed by Western blotting with an anti-PECAM antibody (M-185; Santa Cruz Biotechnology). After the incubation, the proteins absorbed on the Sepharose beads were analyzed by Western blotting with an anti-His<sub>6</sub> antibody (Roche Applied Science) for His-tagged PECAM or an anti-human IgG antibody (Southern Biotech) for Fc-PECAM.

**In Vitro Induction and Quantification of Apoptosis**—Confluent mouse endothelial cells grown on 24-well plates were treated with 0.5  $\mu$ M staurosporine to induce apoptosis (10). At 0, 2, 4, and 8 h after the addition of staurosporine, the cells were measured for their caspase-3/-7 activities using a Caspase-Glo 3/7 assay kit (Promega). Briefly, a luminogenic substrate containing an Asp-Glu-Val-Asp sequence was added and incubated at 37 °C for 1 h, followed by analysis using a multiwell luminometer.

## RESULTS

**PECAM Expression Is Altered by ST6Gal I Deficiency**—Based on previous reports that endothelial cells express significant levels of  $\alpha$ 2,6-linked sialic acid, which are increased by inflammatory cytokines (15, 17), we tried to elucidate a role for  $\alpha$ 2,6-linked sialic acid in endothelial functions. First, we performed immunohistochemical analyses of brain sections from wild-type and ST6Gal I-deficient mice using an anti-ST6Gal I antibody or TJA-I lectin that recognizes Sia $\alpha$ 2,6Gal $\beta$ 1,4GlcNAc residues. In the brain sections from wild-type mice, blood vessels were exclusively detected by TJA-I lectin, because all of the TJA-I positive signals were perfectly matched with those of PECAM as an endothelial marker (Fig. 1A). The specificity of the TJA-I staining was confirmed by the fact that this staining was totally abolished in the brain sections from ST6Gal I-deficient mice (Fig. 1B). Furthermore, we found that ST6Gal I itself was exclusively detected in the blood vessels. Our findings that ST6Gal I products were not present in the brain parenchyma are consistent with a previous report that brain N-glycans predominantly carry  $\alpha$ 2,3-linked sialic acid, with little or no  $\alpha$ 2,6-linked sialic acid (18). Even though ST6Gal I-deficient mice grow normally and exhibit no tissue abnormalities (19), immunostaining of PECAM was also abolished in the brain sections from ST6Gal I-deficient mice (Fig. 1B). We confirmed that PECAM itself contained  $\alpha$ 2,6-linked sialic acid residues added by ST6Gal I, because agarose coupled with the Sia $\alpha$ 2,6-Gal-binding SSA lectin pulled down almost all of the PECAM in tissue lysates from wild-type mice but was unable to pull down PECAM in tissue lysates from ST6Gal I-deficient mice (Fig. 1C), in which PECAM was modified with other types of sialic acids (supplemental Fig. S1). Because the glycosylation-independent anti-PECAM antibody raised against a peptide at the C terminus of PECAM did not stain the brain sections from ST6Gal I-deficient mice (supplemental Fig. S2), defective PECAM glycosylation was not related to this result. On the contrary, the levels of PECAM mRNA were almost the same in the two types of mice (Fig. 1D). Furthermore, Western blot analyses of tissue lysates from ST6Gal I-deficient mice revealed that the total level of PECAM was reduced to only about 70% of the normal level in the lung (Fig. 1E).

**ST6Gal I Expression Increases Cell-surface PECAM Residency**—N-Glycan chain multivalency has been proven to enhance the cell-surface residency of growth-modulating receptors (20). Therefore, we examined whether ST6Gal I overexpression in endothelial cells could enhance the level of cell-surface PECAM. Overexpression of ST6Gal I in HUVECs using an adenovirus method for gene delivery resulted in an  $\sim$ 40% increase in cell-surface  $\alpha$ 2,6-linked

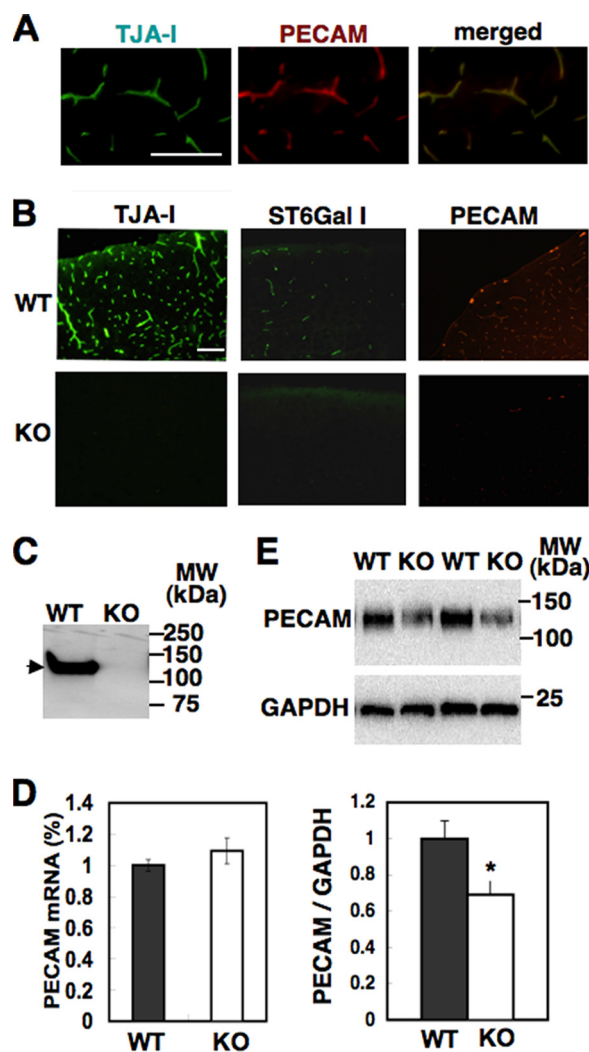


**FIGURE 1. Altered PECAM expression in ST6Gal I-deficient mice.** *A*, brain sections from wild-type mice were stained with the Sia $\alpha$ 2,6Gal-binding TJA-I lectin and an anti-PECAM antibody (MEC13.3) and then observed by confocal fluorescence microscopy. The colocalized staining appears yellow. *B*, brain sections from wild-type (WT) and ST6Gal I-deficient (KO) mice were stained with the TJA-I lectin, an anti-ST6Gal I antibody, and an anti-PECAM antibody (MEC13.3). Scale bars, 200  $\mu$ m. *C*, lung homogenates prepared from wild-type and ST6Gal I-deficient mice were precipitated with SSA-agarose. The precipitated samples were analyzed by Western blotting with an anti-PECAM antibody (M-20). *D*, lung PECAM and GAPDH mRNA levels in wild-type and ST6Gal I-deficient mice were analyzed by real time PCR. The expression levels of PECAM were measured in duplicate and normalized by the corresponding GAPDH expression levels. Data are presented as means  $\pm$  S.E. ( $n = 3$ ). *E*, lung homogenates (10  $\mu$ g of total protein) from wild-type and ST6Gal I-deficient mice were analyzed by immunoblotting with anti-PECAM (M-20) and anti-GAPDH antibodies. The bars represent the relative PECAM immunoreactivities shown as means  $\pm$  S.E. ( $n = 6$ ). \*,  $p < 0.001$ .

sialic acid compared with the control LacZ vector (Fig. 2A). Even though the total PECAM level was not affected by this ST6Gal I overexpression (Fig. 2B), the cell-surface PECAM was increased to  $\sim$ 140% in response to the increased cell-surface  $\alpha$ 2,6-linked sialic acid (Fig. 2, A and C). In addition, PECAM immunoreactivity was detected in tissue sections from ST6Gal I-deficient mice after autoclave treatment for antigen retrieval (supplemental Fig. S2). Because the level of cell-surface VE-cadherin, which contains  $\alpha$ 2,6-linked sialic acid (21), was not affected by ST6Gal I overexpression (Fig. 2C), there appeared to be selectivity for the correlation

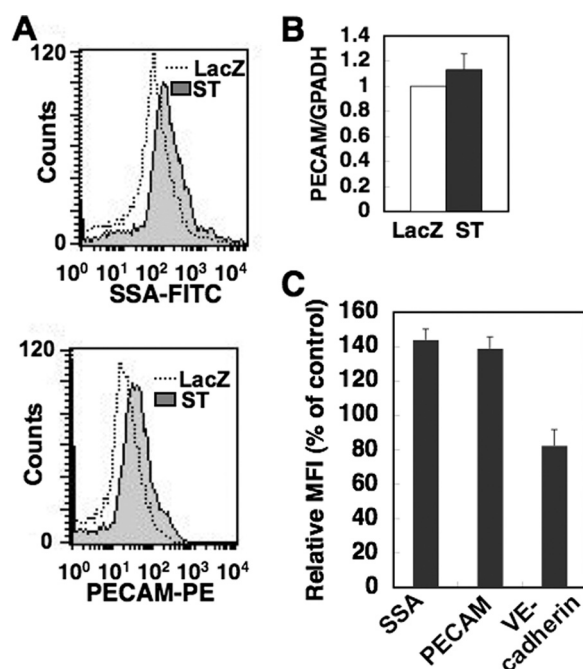


**FIGURE 2. Increased cell-surface expression of PECAM after ST6Gal I expression.** *A*, transfection of HUVECs was achieved by infection with adenovirus preparations of ST6Gal I (ST) or LacZ using 50 plaque-forming units/cell. At 48 h after infection, the cells ( $5 \times 10^5$ ) were detached, resuspended as single-cell suspensions, and probed with SSA-fluorescein isothiocyanate (FITC) or an anti-PECAM-PE antibody. *B*, lysates of HUVECs infected with ST6Gal I adenovirus (ST) or control adenovirus (LacZ) were analyzed by Western blotting using anti-PECAM and anti-GAPDH antibodies. The bars represent the relative immunoreactivities of PECAM to GAPDH shown as means  $\pm$  S.E. ( $n = 3$ ). *C*, cell-surface expressions of  $\alpha$ 2,6-sialic acid (detected by SSA-biotin and Alexa Fluor 488-conjugated streptavidin), PECAM, and VE-cadherin are shown as the mean fluorescence intensities (MFI) in HUVECs infected with ST6Gal I adenovirus or control adenovirus.

between ST6Gal I expression and the cell-surface residency of membrane glycoproteins. To explore the intracellular behavior of endothelial PECAM, we isolated liver sinusoidal endothelial cells from the livers of wild-type and ST6Gal I-deficient mice using an established method (supplemental Fig. S3). Immunostaining analyses revealed that PECAM was localized at the cell borders in the endothelial cells from wild-type mice (Fig. 3A, left panels). In the ST6Gal I-deficient cells, however, this junctional PECAM localization was absent and instead an increased level of intracellular PECAM was colocalized with the early endosome marker EEA-1 (Fig. 3A, right panels) and the late endosome marker lysobisphosphatidic acid (supplemental Fig. S4). These results indicate that more PECAM was endocytosed under ST6Gal I deficiency. After overexpression of ST6Gal I in ST6Gal I-deficient cells, the intracellular PECAM was returned to the cell borders (Fig. 3B). Based on these results, we suspected that the cell-surface half-life of PECAM was decreased, similar to the case for other *N*-glycan mutations in which the cell-surface expressions of growth factor receptors and glucose transporters are greatly diminished under highly branching GlcNAcT glycosyltransferase deficiency (22, 23). The kinetics of the cell-surface retention of PECAM revealed that the PECAM half-life at the cell surface was decreased by 2-fold in the absence of ST6Gal I (Fig. 3C).

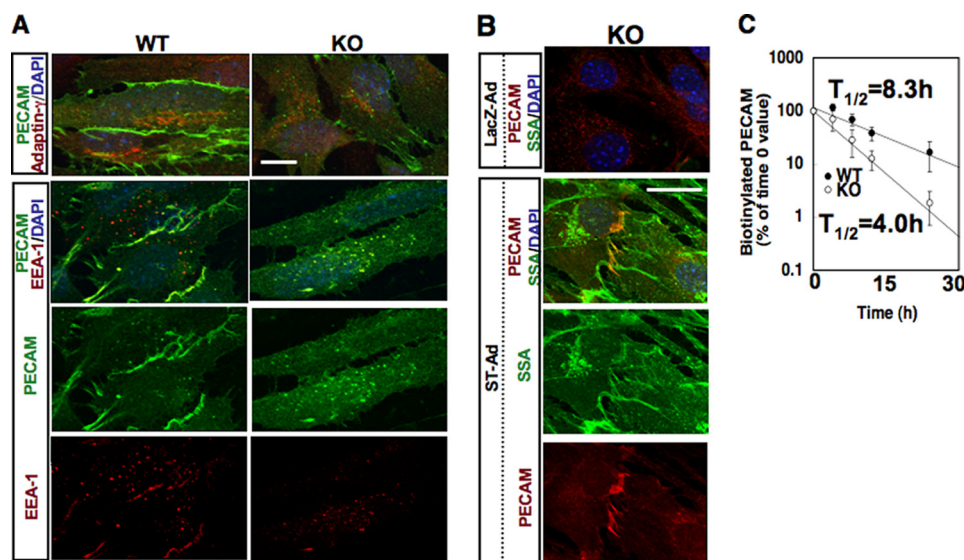


**FIGURE 3. Altered PECAM expression in ST6Gal I-deficient endothelial cells.** *A*, primary liver sinusoidal endothelial cells were prepared from wild-type (*WT*) and ST6Gal I-deficient (*KO*) mice, fixed, and stained with an anti-PECAM antibody (green) and antibodies against a trans-Golgi marker ( $\gamma$ -adaplin; red) or an early endosome marker (*EEA-1*; red). Scale bar, 20  $\mu$ m. *B*, primary liver sinusoidal endothelial cells from ST6Gal I-deficient mice were infected with adenovirus preparations for ST6Gal I (*ST-Ad*) or LacZ (*LacZ-Ad*) using 50 plaque-forming units/cell. 48 h after infection, the cells were fixed and stained with SSA lectin (green), an anti-PECAM antibody (MEC13.3, red), and 4',6-diamidino-2-phenylindole (DAPI) (blue). Scale bar, 20  $\mu$ m. *C*, half-lives of PECAM cell-surface expression on endothelial cells from wild-type and ST6Gal I-deficient mice were determined after cell-surface biotinylation and incubation for 3, 6, 12, and 24 h. Data are presented as the means  $\pm$  S.E. from three separate experiments.

*ST6Gal I* Deficiency Causes Functional Abnormality of PECAM—Even though the precise mechanism by which PECAM transduces inhibitory signals to the cell remains to be determined, an important step appears to be the tyrosine phosphorylation within the immunoreceptor tyrosine-based inhibitory motif of PECAM, which leads to SHP2 recruitment and translocation to cell junctions (7, 10, 24). In ST6Gal I-deficient mice, the level of tyrosine phosphorylation of PECAM was significantly decreased (Fig. 4A) and fewer PECAM·SHP2 complexes were detected (Fig. 4B), implying that ST6Gal I-dependent cell-surface PECAM localization is required for the formation of PECAM·SHP2 complexes to confer cell signaling to endothelial cells. Indeed, the level of phosphotyrosine in the endothelial cells from ST6Gal I-deficient mice was significantly higher than that in the corresponding cells from wild-type mice (Fig. 4C). Even though

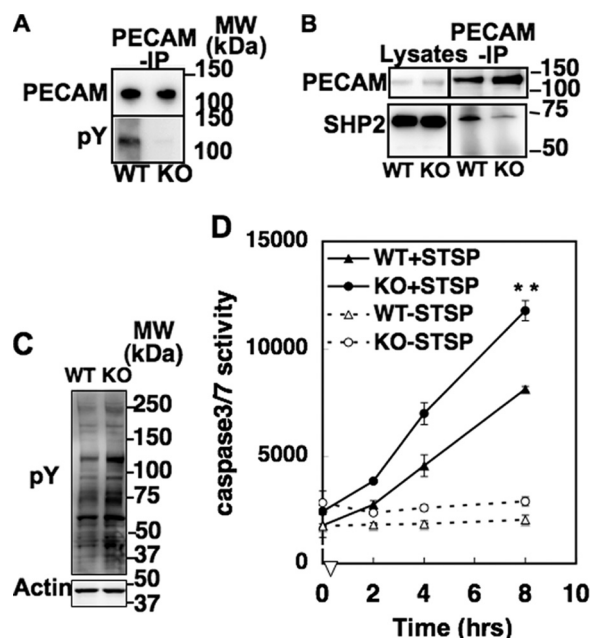


**FIGURE 4. ST6Gal I expression is necessary for PECAM to transduce inhibitory signals.** *A* and *B*, PECAM complexes were precipitated from lung lysates from wild-type (*WT*) and ST6Gal I-deficient (*KO*) mice using an anti-PECAM antibody and analyzed with anti-PECAM and anti-phosphotyrosine (pY) antibodies (*A*) or anti-SHP2 antibodies (*B*). *C*, endothelial cell lysates (20  $\mu$ g of protein) from wild-type and ST6Gal I-deficient mice were analyzed by Western blotting using an anti-phosphotyrosine (pY) antibody. *D*, primary liver sinusoidal endothelial cells from the livers of wild-type and ST6Gal I-deficient mice were grown on 96-well plates. At 0, 2, 4, and 8 h after the addition of staurosporine (*STSP*), the cells were measured for their caspase-3/-7 activities using a multiwell luminometer. Data are presented as the means  $\pm$  S.E. from three separate experiments. \*\*,  $p < 0.0005$ , versus ST6Gal I-deficient mice. *IP*, immunoprecipitated.

PECAM is regarded as a multifunctional molecule (6, 25), several reports have highlighted that PECAM functions as an inhibitor of mitochondrion-dependent apoptosis (8–10). We therefore speculated that ST6Gal I deficiency would increase the sensitivity of endothelial cells to mitochondrion-dependent apoptotic stimuli, because of the lack of functional PECAM. To directly examine whether ST6Gal I-deficient endothelial cells were more sensitive to apoptotic stimuli, we treated endothelial cells from wild-type and ST6Gal I-deficient mice with staurosporine, a trigger for mitochondrion-dependent apoptosis. The ST6Gal-deficient endothelial cells were indeed more sensitive to staurosporine treatment than the wild-type endothelial cells (Fig. 4D).

*Sialic Acid-dependent Homophilic PECAM Interactions*—Given that cell-surface retention of PECAM is greatly decreased by ST6Gal I deficiency, it is possible that an  $\alpha$ ,6-linked sialic acid-binding protein exists at the cell surface. It is generally accepted that the cell-surface residency of glycoproteins is partly supported by galectin, a galactose-binding protein (20). Nevertheless, recognition of *N*-glycans by galectin was found to be disrupted by modification of *N*-glycans by ST6Gal I (26–28). A well known  $\alpha$ ,2,6-linked sialic acid-recognizing Ig superfamily member, CD22, is restricted to the B-cell lineage (29–32). Because accumulating data support the idea that PECAM homophilic interactions are requisite for its proper functions (8, 33), we speculated that sialic acids would mediate homophilic PECAM interactions. Consequently, we performed *in vitro* assays using Fc-tagged PECAM (PECAM-Fc) and His-tagged PECAM (PECAM-His). Fc-PECAM immobilized onto protein A-Sepharose was able to pull down PECAM-His, and this interaction was abolished by sialidase treatment of either or

## Sialic Acid-dependent Homophilic PECAM Interactions

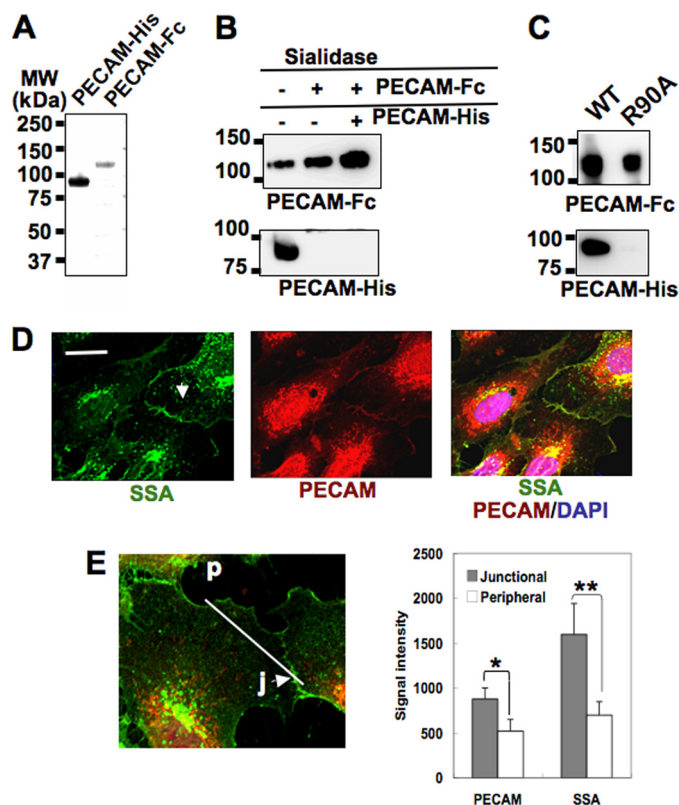


**FIGURE 5. Sialic acid-based homophilic PECAM interactions.** *A*, purities of PECAM-Fc and PECAM-His were verified by silver staining. *B*, PECAM-Fc adsorbed to protein A-Sepharose was incubated with His-tagged PECAM in the presence or absence of *V. cholerae* sialidase. Alternatively, sialidase-treated PECAM-Fc was incubated with PECAM-His. The absorbed proteins on the protein A-Sepharose were analyzed by Western blotting with anti-human IgG antibody (for PECAM-Fc) or anti-His antibody (for PECAM-His). *C*, after PECAM-Fc (WT) or PECAM<sub>R90A</sub>-Fc (R90A) was incubated with PECAM-His, the absorbed proteins on the protein A-Sepharose were analyzed by Western blotting. *D*, HUVECs were stained with SSA lectin and an anti-PECAM antibody (H-200). Scale bar, 20  $\mu$ m. *E*, fluorescence intensity profiles were taken along the line shown in the image of HUVECs stained with SSA lectin and an anti-PECAM antibody. The bars represent the signal intensities of the PECAM and SSA epitopes at junctional (j) and peripheral (p) areas shown as means  $\pm$  S.E. ( $n = 6$ ). \*,  $p < 0.005$ ; \*\*,  $p < 0.05$ . DAPI, 4,6-diamidino-2-phenylindole.

both PECAM-Fc and PECAM-His, or only PECAM-Fc (Fig. 5, *A* and *B*), thereby providing direct evidence of sialic acid-dependent homophilic PECAM interactions. Because a conserved Arg in the N-terminal Ig domain is essential in sialic acid recognition by Siglec (34), we constructed the PECAM mutant, PECAM<sub>R90A</sub>, in which highly conserved Arg-90 in the first Ig domain was replaced with Ala. Homophilic interaction of PECAM was markedly lost in the PECAM<sub>R90A</sub>-Fc mutant (Fig. 5C), indicating that Arg-90 is an interaction site on PECAM. When we stained HUVECs with SSA lectin and an anti-PECAM antibody, both the SSA epitopes and PECAM were more concentrated at cell-cell junctions than in the peripheral regions (Fig. 5, *D* and *E*), further suggesting a role for  $\alpha$ 2,6-sialic acid in the PECAM interactions.

## DISCUSSION

Based on our present findings, a model for sialic acid-dependent homophilic PECAM interactions was developed (Fig. 6). PECAM with normal sialic acids mediates homophilic interactions at the cell surface to recruit SHP2 phosphatase to trans-

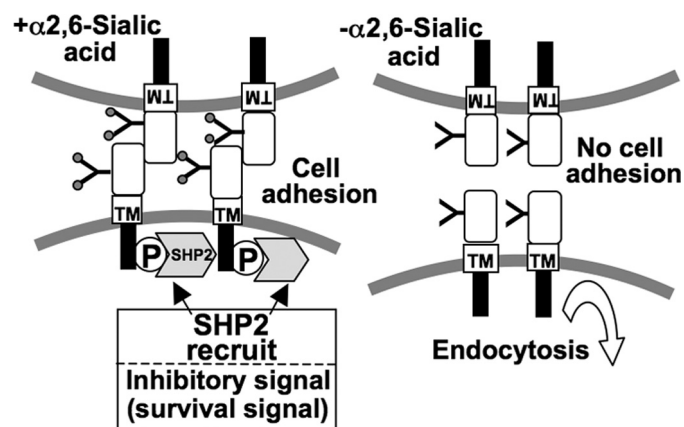


**FIGURE 6. Schematic diagrams of a model for sialic acid-dependent homophilic PECAM interactions.** PECAM proteins modified with sialic acids interact with one another at the cell surface, and subsequently recruit SHP2 to transduce inhibitory signals to the cell (*left*). Without the sialic acids, PECAM fails to mediate the homophilic interactions required for the underlying signal transduction (*right*). TM, transmembrane.

duce inhibitory signals, such as antiapoptotic signals, to the cell. Under ST6Gal I deficiency, PECAM fails to mediate homophilic interactions, thus leading to an inability to transduce signals to the cell. As an underlying mechanism of the sialic acid-based homophilic PECAM interactions, we speculated that PECAM itself would be an  $\alpha$ 2,6-linked sialic acid-binding protein because PECAM also belongs to the Ig superfamily that includes a subfamily of sialic acid-binding Ig-like lectins (Siglecs). Even though PECAM is not likely to possess an N-terminal V-set Ig domain that plays a role in sialic acid binding in Siglec (34), replacement of conserved Arg-90 in the first Ig domain of PECAM with Ala greatly reduced the homophilic binding activity, indicating that Arg-90 is an interaction site of PECAM. A detailed molecular structural study to elucidate how and which part of PECAM exhibits its sialic acid-binding activity is a challenging issue for the future.

Endothelial cells from ST6Gal I-deficient mice show an overlapping phenotype with the corresponding cells from PECAM-deficient mice, in terms of their increased sensitivity to mitochondrion-dependent apoptotic stimuli (8–10). Interestingly, stressed conditions enhance the endothelial cell-surface expression of PECAM without changing the level of PECAM mRNA, thereby leading to enhanced cell survival signals (12). Glycan modification of PECAM may be responsible for regulating various pathological situations. Nevertheless, because ST6Gal I acts on various endothelial glycoproteins, the identification of key molecules other than PECAM whose functions are regulated by ST6Gal I remains one of our ongoing projects. Finally, our findings that ST6Gal I-deficient endothelial cells exhibit increased sensitivity to apoptotic signals provide new possibilities for the development of glycan-targeted antiangiogenesis strategies.

**Acknowledgments**—We thank Dr. Jing Sun (University of Pennsylvania School of Medicine, Philadelphia) for the mouse PECAM pcDNA, Dr. Toshihide Kobayashi (RIKEN ASI) for the anti-lysobisphosphatidic acid antibody, and Dr. Yoshihiro Yoshihara (RIKEN BSI Institute) for pEF-Fc.

## REFERENCES

- Carmeliet, P. (2005) *Nature* **438**, 932–936
- Folkman, J. (2007) *Nat. Rev. Drug Discov.* **6**, 273–286
- Ferrara, N., Hillan, K. J., Gerber, H. P., and Novotny, W. (2004) *Nat. Rev. Drug Discov.* **3**, 391–400
- Olsson, A. K., Dimberg, A., Kreuger, J., and Claesson-Welsh, L. (2006) *Nat. Rev. Mol. Cell Biol.* **7**, 359–371
- Tzima, E., Irani-Tehrani, M., Kiosses, W. B., Dejana, E., Schultz, D. A., Engelhardt, B., Cao, G., DeLisser, H., and Schwartz, M. A. (2005) *Nature* **437**, 426–431
- Newman, P. J., and Newman, D. K. (2003) *Arterioscler. Thromb. Vasc. Biol.* **23**, 953–964
- Newman, P. J., Berndt, M. C., Gorski, J., White, G. C., 2nd, Lyman, S., Paddock, C., and Muller, W. A. (1990) *Science* **247**, 1219–1222
- Bird, I. N., Taylor, V., Newton, J. P., Spragg, J. H., Simmons, D. L., Salmon, M., and Buckley, C. D. (1999) *J. Cell Sci.* **112**, 1989–1997
- Noble, K. E., Wickremasinghe, R. G., DeCornet, C., Panayiotidis, P., and Yong, K. L. (1999) *J. Immunol.* **162**, 1376–1383
- Gao, C., Sun, W., Christofidou-Solomidou, M., Sawada, M., Newman, D. K., Bergom, C., Albelda, S. M., Matsuyama, S., and Newman, P. J. (2003) *Blood* **102**, 169–179
- Ferrero, E., Belloni, D., Contini, P., Foglieni, C., Ferrero, M. E., Fabbri, M., Poggi, A., and Zocchi, M. R. (2003) *Blood* **101**, 186–193
- Limaye, V., Li, X., Hahn, C., Xia, P., Berndt, M. C., Vadas, M. A., and Gamble, J. R. (2005) *Blood* **105**, 3169–3177
- Zhou, Z., Christofidou-Solomidou, M., Garlanda, C., and DeLisser, H. M. (1999) *Angiogenesis* **3**, 181–188
- Nitschke, L., Floyd, H., Ferguson, D. J., and Crocker, P. R. (1999) *J. Exp. Med.* **189**, 1513–1518
- Hanasaki, K., Varki, A., Stamenkovic, I., and Bevilacqua, M. P. (1994) *J. Biol. Chem.* **269**, 10637–10643
- Sugimoto, I., Futakawa, S., Oka, R., Ogawa, K., Marth, J. D., Miyoshi, E., Taniguchi, N., Hashimoto, Y., and Kitazume, S. (2007) *J. Biol. Chem.* **282**, 34896–34903
- Hanasaki, K., Varki, A., and Powell, L. D. (1995) *J. Biol. Chem.* **270**, 7533–7542
- Kleene, R., and Schachner, M. (2004) *Nat. Rev. Neurosci.* **5**, 195–208
- Hennet, T., Chui, D., Paulson, J. C., and Marth, J. D. (1998) *Proc. Natl. Acad. Sci. U.S.A.* **95**, 4504–4509
- Lau, K. S., Partridge, E. A., Grigorian, A., Silvescu, C. I., Reinhold, V. N., Demetriou, M., and Dennis, J. W. (2007) *Cell* **129**, 123–134
- Geyer, H., Geyer, R., Odenthal-Schnittler, M., and Schnittler, H. J. (1999) *Glycobiology* **9**, 915–925
- Partridge, E. A., Le Roy, C., Di Guglielmo, G. M., Pawling, J., Cheung, P., Granovsky, M., Nabi, I. R., Wrana, J. L., and Dennis, J. W. (2004) *Science* **306**, 120–124
- Ohtsubo, K., Takamatsu, S., Minowa, M. T., Yoshida, A., Takeuchi, M., and Marth, J. D. (2005) *Cell* **123**, 1307–1321
- Osawa, M., Masuda, M., Kusano, K., and Fujiwara, K. (2002) *J. Cell Biol.* **158**, 773–785
- Woodfin, A., Voisin, M. B., and Nourshargh, S. (2007) *Arterioscler. Thromb. Vasc. Biol.* **27**, 2514–2523
- Amano, M., Galvan, M., He, J., and Baum, L. G. (2003) *J. Biol. Chem.* **278**, 7469–7475
- Cha, S. K., Ortega, B., Kurosu, H., Rosenblatt, K. P., Kuro-O, M., and Huang, C. L. (2008) *Proc. Natl. Acad. Sci. U.S.A.* **105**, 9805–9810
- Zhuo, Y., Chammass, R., and Bellis, S. L. (2008) *J. Biol. Chem.* **283**, 22177–22185
- Powell, L. D., Sgroi, D., Sjoberg, E. R., Stamenkovic, I., and Varki, A. (1993) *J. Biol. Chem.* **268**, 7019–7027
- Poe, J. C., Fujimoto, Y., Hasegawa, M., Haas, K. M., Miller, A. S., Sanford, I. G., Bock, C. B., Fujimoto, M., and Tedder, T. F. (2004) *Nat. Immunol.* **5**, 1078–1087
- Grewal, P. K., Boton, M., Ramirez, K., Collins, B. E., Saito, A., Green, R. S., Ohtsubo, K., Chui, D., and Marth, J. D. (2006) *Mol. Cell. Biol.* **26**, 4970–4981
- Collins, B. E., Smith, B. A., Bengtson, P., and Paulson, J. C. (2006) *Nat. Immunol.* **7**, 199–206
- Newton, J. P., Buckley, C. D., Jones, E. Y., and Simmons, D. L. (1997) *J. Biol. Chem.* **272**, 20555–20563
- Crocker, P. R., and Varki, A. (2001) *Trends Immunol.* **22**, 337–342